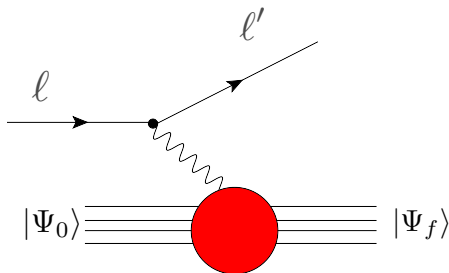


Comparisons to electron-scattering

Noemi Rocco, L. Alvarez Ruso, O. Benhar, A. Lovato, J. Nieves



“Theoretical Developments in ν -Nucleus Scattering”

INT Workshop INT-16-63W
December 5 - 9, 2016



- 1 Contribution of one- and two-body currents to electron-nucleus interactions within the Spectral Function approach
- 2 Comparison of the results obtained for electron-nucleus scattering within the Spectral Function and the Green's Function Monte Carlo approaches
- 3 Analysis of the (super)scaling features of the Green's Function Monte Carlo results

- 1 Contribution of one- and two-body currents to electron-nucleus interactions within the Spectral Function approach
- 2 Comparison of the results obtained for electron-nucleus scattering within the Spectral Function and the Green's Function Monte Carlo approaches
- 3 Analysis of the (super)scaling features of the Green's Function Monte Carlo results

- 1 Contribution of one- and two-body currents to electron-nucleus interactions within the Spectral Function approach
- 2 Comparison of the results obtained for electron-nucleus scattering within the Spectral Function and the Green's Function Monte Carlo approaches
- 3 Analysis of the (super)scaling features of the Green's Function Monte Carlo results

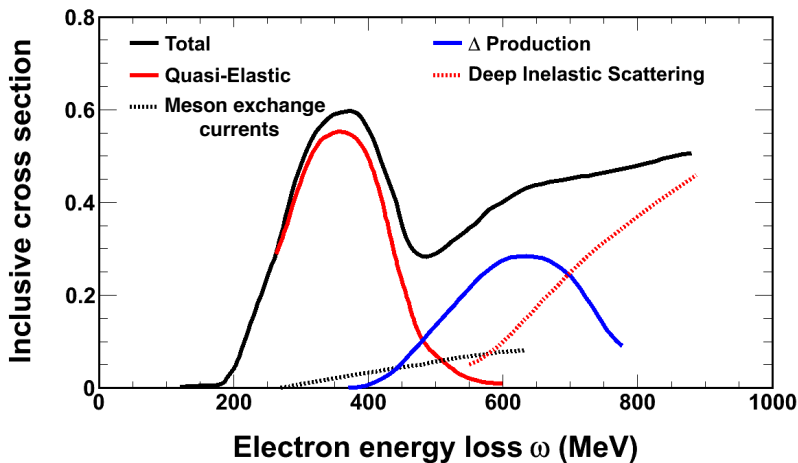
- Understanding neutrino-nucleus interactions in the broad kinematical region relevant to long-baseline neutrino-oscillation experiments is a challenging many-body problem. It requires an accurate description of both nuclear dynamics and of the interaction vertex
- To validate our models it is important to check the results using the large amount of electron scattering data
- *Ab initio* methods can provide strict benchmarks, valuable to constrain more approximate models in the limit of moderate momentum transfer

- Understanding neutrino-nucleus interactions in the broad kinematical region relevant to long-baseline neutrino-oscillation experiments is a challenging many-body problem. It requires an accurate description of both nuclear dynamics and of the interaction vertex
- To validate our models it is important to check the results using the large amount of electron scattering data
- *Ab initio* methods can provide strict benchmarks, valuable to constrain more approximate models in the limit of moderate momentum transfer

- Understanding neutrino-nucleus interactions in the broad kinematical region relevant to long-baseline neutrino-oscillation experiments is a challenging many-body problem. It requires an accurate description of both nuclear dynamics and of the interaction vertex
- To validate our models it is important to check the results using the large amount of electron scattering data
- *Ab initio* methods can provide strict benchmarks, valuable to constrain more approximate models in the limit of moderate momentum transfer

Inclusive lepton-nucleus cross section at fixed beam energy

Inclusive electron-nucleus cross section at $E_e \sim 1$ GeV, as a function of ω .



The different reaction mechanisms, contributing to the cross section at different values of ω , can be easily identified.

The electron-nucleus x-section

- The double differential x-section of the process $e^- + A \rightarrow e^- + X$, can be written as

$$\frac{d^2\sigma}{d\Omega_{\mathbf{k}'} dk'_0} = \frac{\alpha^2}{Q^4} \frac{E'_e}{E_e} L_{\mu\nu} W_A^{\mu\nu} .$$

- $L_{\mu\nu}$ is completely determined by the lepton kinematics
- The hadronic tensor describes the **response** of the target nucleus.

$$W_A^{\mu\nu} = \sum_X \langle 0 | J_A^{\mu\dagger} | X \rangle \langle X | J_A^\nu | 0 \rangle \delta^{(4)}(p_0 + q - p_X) ,$$

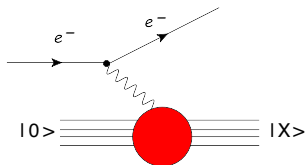
initial state

$$|0\rangle ; p_0$$

final state

$$|X\rangle = |1p; 1h\rangle, |2p; 2h\rangle \dots ; p_X$$

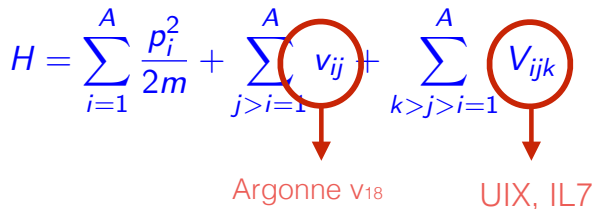
Non relativistic nuclear many-body theory (NMBT) provides a fully consistent theoretical approach allowing for an accurate description of $|0\rangle$, independent on momentum transfer.



Limit of moderate $|q|$ ($\lesssim 500$ MeV)

- Within NMBT the nucleus is described as a collection of A pointlike nucleons, the dynamics of which are described by the nonrelativistic Hamiltonian

$$H = \sum_{i=1}^A \frac{p_i^2}{2m} + \sum_{j>i=1}^A v_{ij} + \sum_{k>j>i=1}^A V_{ijk}$$



Argonne v_{18} UIX, IL7

- Initial state definition:

$$H|0\rangle = E_0|0\rangle$$

- Final state definition

$$H|X\rangle = E_X|X\rangle$$

The above Schrödinger equation can only be exactly solved for the ground- and low-lying excited states of nuclei with $A \leq 12$.

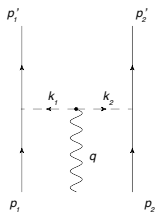
The nuclear current operator

- The nuclear Hamiltonian does not commute with the charge density operator: $[H, J^0] \neq 0$
- In order for the continuity equation to be satisfied two body currents are needed:

$$\frac{\partial}{\partial t} J^0 + \vec{\nabla} \cdot \vec{J} = 0$$

- The nuclear current includes one-and two-nucleon contributions

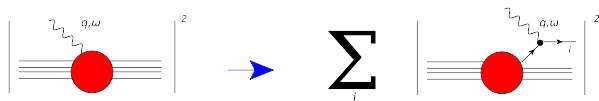
$$J_A^\mu(q) = \sum_{i=1}^A j_i^\mu(q) + \sum_{j>i=1}^A j_{ij}^\mu(q_1, q_2) \delta(q - q_1 - q_2)$$



- non relativistic reduction of the current (q/m expansions) .

The factorization “paradigm”

- Simplest implementation: **Impulse Approximation (IA)**



- At $|\mathbf{q}|^{-1} \ll d$:

$$J_A^\mu \longrightarrow \sum_i j_i^\mu, \quad |X\rangle \longrightarrow |x, \mathbf{p}_x\rangle \otimes |R, \mathbf{p}_R\rangle,$$

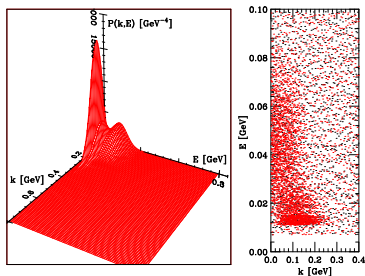
- The nuclear cross section can be traced back to the one describing the interaction with individual bound nucleons

$$d\sigma_A = \int dE d^3k d\sigma_N P(k, E)$$

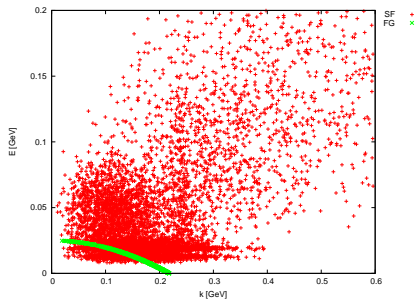
- ▶ An integration on the nucleon momentum and removal energy is carried out, with a weight given by the **Spectral Function**

Spectral function and energy-momentum distribution

- ▶ Oxygen spectral function, obtained within LDA.



- ▶ Momentum and removal energy sampled from LDA (red) and RFGM (green) oxygen spectral functions



$$P_{LDA}(\mathbf{p}, E) = P_{MF}(\mathbf{p}, E) + P_{CORR}(\mathbf{p}, E)$$

$$\sum_{n \in (F)} Z_n |\phi_n(\mathbf{p})|^2 F_n(E - E_n) \quad \int d^3r \varrho_A(\mathbf{r}) P_{CORR}^{NM}(\mathbf{p}, E; \varrho = \varrho_A(\mathbf{r}))$$

- Scattering off high momentum and high removal energy nucleons, providing $\sim 20\%$ of the total strength.

Convolution scheme

$$\frac{d\sigma^{\text{FSI}}}{d\omega d\Omega} = \int d\omega' f_{\mathbf{q}}(\omega - \omega') \frac{d\sigma^{\text{IA}}}{d\omega d\Omega}$$

The folding function can be decomposed in the form

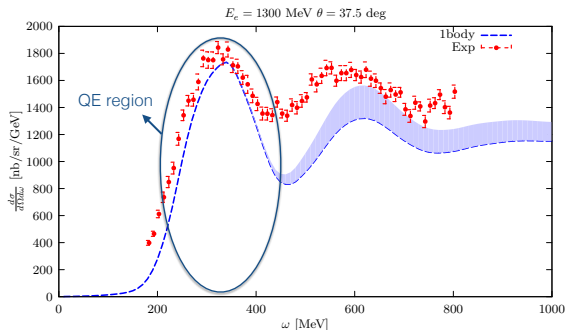
$$f_{\mathbf{q}}(\omega) = \delta(\omega) \sqrt{T_A} + (1 - \sqrt{T_A}) F_{\mathbf{q}}(\omega)$$

showing that the strength of FSI is driven by

- ▶ the nuclear transparency T_A
- ▶ the finite-width function $F_{\mathbf{q}}(\omega)$
- A. Ankowski *et al.*, Phys. Rev. D 91, 033005 (2015)
- O. Benhar, Phys. Rev. C 87, 024606 (2013).

Range of applicability of the IA

- Electron-Carbon cross section for $E_e = 1.3$ GeV, $\theta_e = 37.5$.

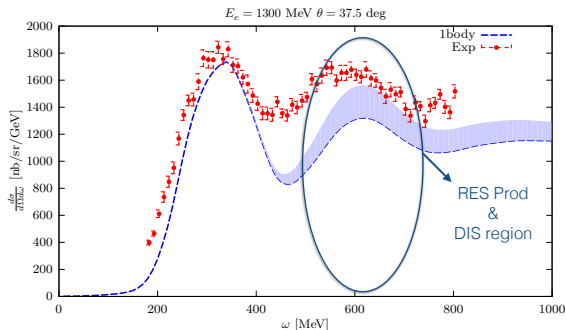


$$\tilde{W}_1^N = \tau G_{MN}^2 \delta\left(\tilde{\omega} + \frac{\tilde{q}^2}{2m}\right),$$

$$\tilde{W}_2^N = \frac{1}{(1 + \tau)} \left(G_{EN}^2 + \tau G_{MN}^2 \right) \delta\left(\tilde{\omega} + \frac{\tilde{q}^2}{2m}\right)$$

Range of applicability of the IA

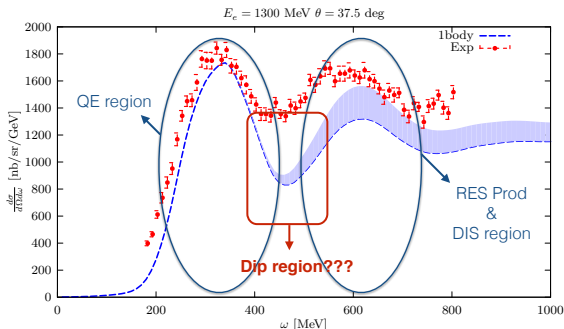
- Electron-Carbon cross section for $E_e = 1.3$ GeV, $\theta_e = 37.5$.



The inelastic nucleon structure functions are extracted from the analysis of electron-proton and electron-deuteron scattering data (Bodek-Ritchie).

Range of applicability of the IA

- Electron-Carbon cross section for $E_e = 1.3$ GeV, $\theta_e = 37.5$.

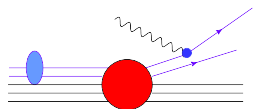


- The contribution of two-body currents has to be included. These are expected to play a significant role in the so called *dip region*.

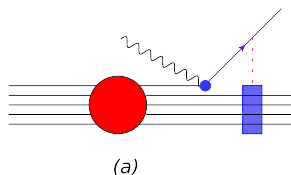
How can $2p2h$ final states be produced?

In a model accounting for NN correlations, $2p2h$ final states can be produced through 3 different reaction mechanisms.

- Initial State Correlations (ISC):

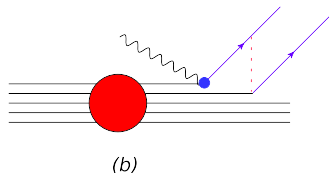
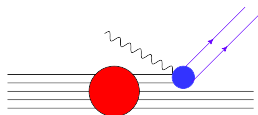


- Final State Interactions (FSI):



(a)

- Meson Exchange Currents (MEC):



(b)

1p1h and 2p2h contributions to the nuclear cross section

- ▶ The factorization scheme allows for a clear identification of the 1p1h and 2p2h contributions

$$d\sigma = d\sigma_{1p1h} + d\sigma_{2p2h} \propto L_{\mu\nu} (W_{1p1h}^{\mu\nu} + W_{2p2h}^{\mu\nu})$$

- ▶ 2p2h response tensor

$$W_{2p2h}^{\mu\nu} = \sum_{h,h' < k_F} \sum_{p,p' > k_F} \langle 0 | J^{\mu\dagger} | \mathbf{h}\mathbf{h}'\mathbf{p}\mathbf{p}' \rangle \langle \mathbf{h}\mathbf{h}'\mathbf{p}\mathbf{p}' | J^\nu | 0 \rangle \\ \times \delta(\omega + E_0 - E_{hh'pp'}) \delta(\mathbf{q} + \mathbf{h} + \mathbf{h}' - \mathbf{p} - \mathbf{p}') ,$$

- ▶ Current operator in momentum space:

$$J^\mu(\mathbf{k}_1, \mathbf{k}_2) = j_1^\mu(\mathbf{k}_1)\delta(\mathbf{k}_2) + j_2^\mu(\mathbf{k}_2)\delta(\mathbf{k}_1) + j_{12}^\mu(\mathbf{k}_1, \mathbf{k}_2) ,$$

$$W_{2p2h}^{\mu\nu} = W_{2p2h,11}^{\mu\nu} + W_{2p2h,22}^{\mu\nu} + W_{2p2h,12}^{\mu\nu}$$

- 1 Initial state correlations
- 2 MEC, two-body response
- 3 Interference

Initial state correlations

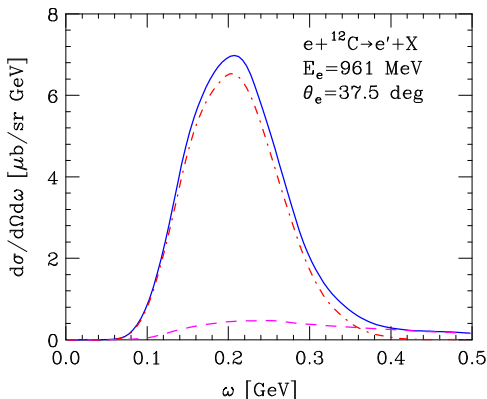
Within the IA...

$$W_{2p2h,11}^{\mu\nu} = \int d^3k \int dE P_{2h1p}(\mathbf{k}, E) \langle k | j_1^\mu | p \rangle \langle p | j_1^\nu | k \rangle \delta(\tilde{\omega} + e_k - e_p)$$

$$P_{2h1p}(\mathbf{k}, E) = \sum_{h, h' < k_F} \sum_{p' > k_F} |\Phi_k^{hh'p'}|^2$$

$\times \delta(E + e_h + e_{h'} - e_{p'})$,

- appearance of the tail of the cross section, extending to large energy loss. This contribution amounts to $\sim 10\%$ of the integrated spectrum.



Production of 2p2h final states

- 1 Initial state correlations
- 2 **MEC, two-body response**
- 3 Interference

Extending the factorization scheme

- Using relativistic MEC and a realistic description of the nuclear ground state requires the extension of the factorization scheme to two-nucleon emission amplitude

- ▶ Rewrite the hadronic final state $|X\rangle$ in the factorized form:

$$|X\rangle \longrightarrow |\mathbf{p} \mathbf{p}'\rangle \otimes |n_{(A-2)}\rangle = |n_{(A-2)}; \mathbf{p} \mathbf{p}'\rangle ,$$

where $|n_{(A-2)}\rangle$ describes the spectator $(A - 2)$ -nucleon system, carrying momentum \mathbf{p}_n .

- ▶ The two nucleon current simplifies

$$\langle X | j_{ij}^\mu | 0 \rangle \rightarrow \int d^3k d^3k' M_n(\mathbf{k}, \mathbf{k}') \langle \mathbf{p} \mathbf{p}' | j_{ij}^\mu | \mathbf{k} \mathbf{k}' \rangle \delta(\mathbf{k} + \mathbf{k}' - \mathbf{p}_n) ,$$

- ▶ The nuclear amplitude: $M_n(\mathbf{k}, \mathbf{k}') = \langle n_{(A-2)}; \mathbf{k} \mathbf{k}' | 0 \rangle$ is independent of \mathbf{q} , and can therefore be obtained within NMBT.

Two nucleon spectral function

- Two-nucleon spectral function of uniform and isospin nuclear matter

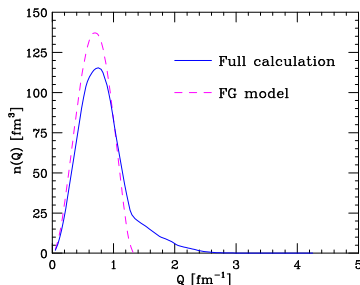
$$P(\mathbf{k}, \mathbf{k}', E) = \sum_n |M_n(\mathbf{k}, \mathbf{k}')|^2 \delta(E + E_0 - E_n)$$

$$n(\mathbf{k}, \mathbf{k}') = \int dE P(\mathbf{k}, \mathbf{k}', E)$$

- Relative momentum distribution

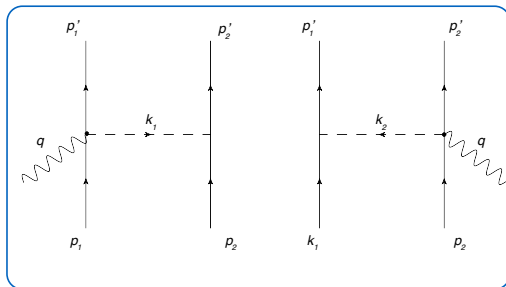
$$n(\mathbf{Q}) = 4\pi |\mathbf{Q}|^2 \int d^3K n\left(\mathbf{Q} + \frac{\mathbf{K}}{2}, \mathbf{Q} - \frac{\mathbf{K}}{2}\right)$$

$$\mathbf{K} = \mathbf{k} + \mathbf{k}' \quad , \quad \mathbf{Q} = \frac{\mathbf{k} - \mathbf{k}'}{2} .$$

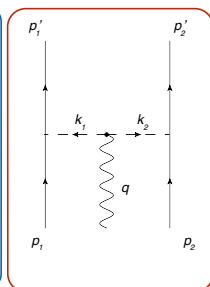


- ▶ Correlation effects lead to **a quenching of the peak** of the distributions and **an enhancement of the high momentum tail**

MEC: Pion exchange

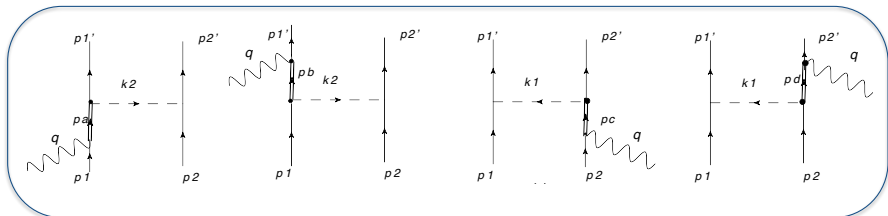


Seagull
or
contact
term



Pion
in
flight
term

MEC: Δ -isobar exchange



The Rarita-Schwinger (RS) expression for the Δ propagator reads

$$S^{\beta\gamma}(p, M_\Delta) = \frac{\not{p} + M_\Delta}{p^2 - M_\Delta^2} \left(g^{\beta\gamma} - \frac{\gamma^\beta \gamma^\gamma}{3} - \frac{2p^\beta p^\gamma}{3M_\Delta^2} - \frac{\gamma^\beta p^\gamma - \gamma^\gamma p^\beta}{3M_\Delta} \right)$$

WARNING

If the condition $p_\Delta^2 > (m_N + m_\pi)^2$ the real resonance mass has to be replaced by $M_\Delta \rightarrow M_\Delta - i\Gamma(s)/2$ where $\Gamma(s) = \frac{(4f_{\pi N\Delta})^2}{12\pi m_\pi^2} \frac{k^3}{\sqrt{s}} (m_N + E_k)$.

2p-2h Transverse Response of nuclear matter

From the 2p-2h hadron tensor...

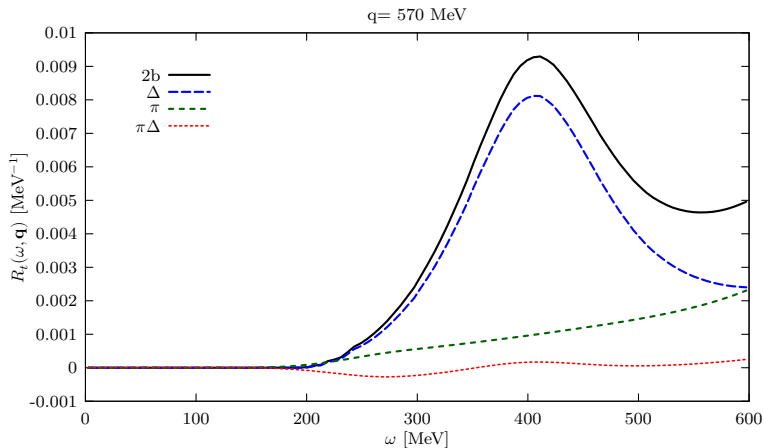
$$W_{2p2h,22}^{\mu\nu} = \int d^3k d^3k' d^3p d^3p' \int dE P_{2h}(\mathbf{k}, \mathbf{k}', E) \langle \mathbf{k}\mathbf{k}' | j_{12}^{\mu} | \mathbf{p}\mathbf{p}' \rangle \langle \mathbf{p}\mathbf{p}' | j_{12}^{\nu} | \mathbf{k}\mathbf{k}' \rangle \\ \times \delta(\mathbf{k} + \mathbf{k}' + \mathbf{q} - \mathbf{p} - \mathbf{p}') \delta(\omega - E - e_p - e_{p'}) \theta(|\mathbf{p}| - k_F) \theta(|\mathbf{p}'| - k_F) .$$

$$P_{2h}(\mathbf{k}, \mathbf{k}', E) = \sum_{h,h' < k_F} |\Phi_{kk'}^{hh'}|^2 \delta(E + e_h + e_{h'})$$

- ▶ 12D integral, can be analytically reduced to a 7D integral → [Monte Carlo integration technique](#)
- ▶ both the direct and Pauli exchange contribution have to be considered (more than 100,000 terms) → [Mathematica and Fortran code](#)

Contribution of the MEC to the transverse response

Separate contributions to the transverse response function $R_T(\omega, q)$ at $q = 570$ MeV: pionic, pionic- Δ interference, Δ and total.



Production of 2p2h final states

- 1 Initial state correlations
- 2 MEC, two-body response
- 3 **Interference**

It cannot be written in terms of SF...

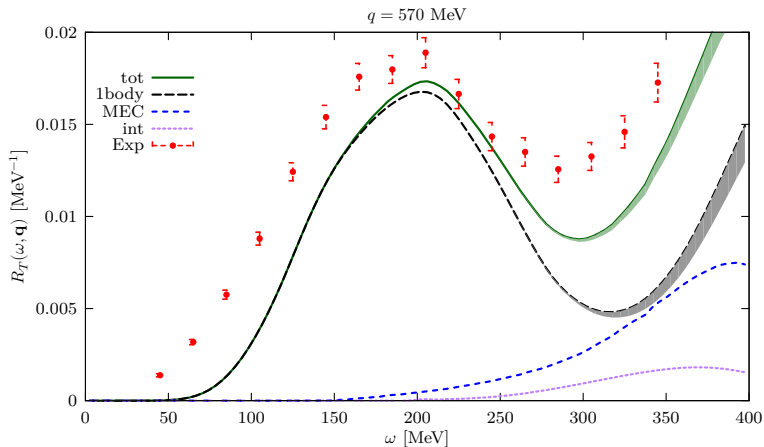
$$\begin{aligned} W^{\mu\nu}_{2p2h,12} = & \int d^3k d^3\xi d^3\xi' d^3h d^3h' d^3p d^3p' \phi_{\xi\xi'}^{hh'*} \left[\Phi_k^{hh'p'} \langle \mathbf{k} | j_1^\mu | \mathbf{p} \rangle \right. \\ & \left. + \Phi_k^{hh'p'} \langle \mathbf{k} | j_2^\mu | \mathbf{p}' \rangle \right] \langle \mathbf{p}, \mathbf{p}' | j_{12}^\nu | \xi, \xi' \rangle \delta(\mathbf{h} + \mathbf{h}' + \mathbf{q} - \mathbf{p} - \mathbf{p}') \\ & \times \delta(\omega + e_h + e_{h'} - e_p - e_{p'}) \theta(|\mathbf{p}| - k_F) \theta(|\mathbf{p}'| - k_F) + \text{h.c.} . \end{aligned}$$

Additional difficulty... This term involves the product of nuclear amplitudes entering in $P(k, E)$ and $P(k, k', E)$

WARNING

This interference contribution would be zero if correlations were not accounted for!

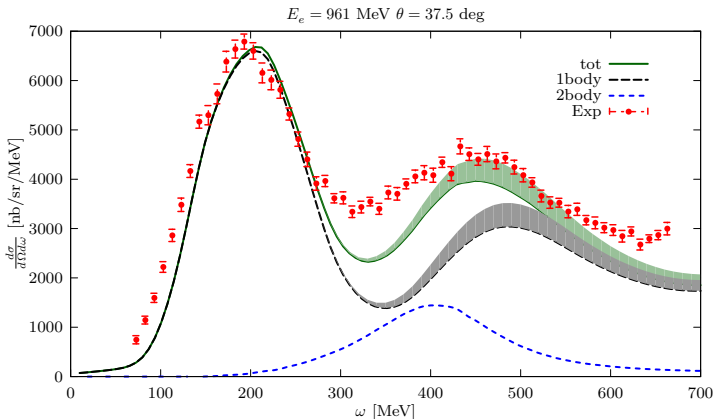
^{12}C electromagnetic response



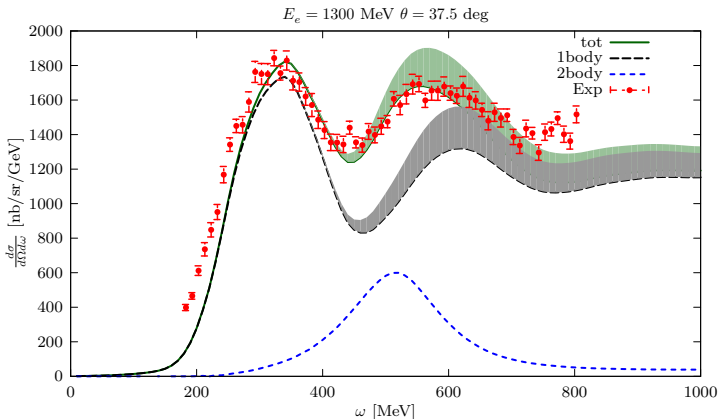
^{12}C calculations indicate a sizable enhancement of the electromagnetic transverse response.

The x-section can be rewritten in terms of R_T and R_L such as

$$\frac{d\sigma}{dE'_e d\Omega} = \sigma_{Mott} \left[\left(\frac{q^2}{\mathbf{q}^2} \right)^2 R_L + \left(\frac{-q^2}{2\mathbf{q}^2} + \tan^2 \frac{\theta}{2} \right) R_T \right]$$

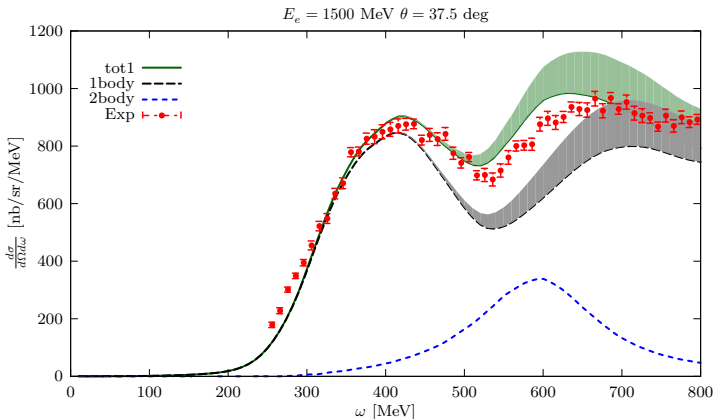


$e^- - {}^{12}\text{C}$ inclusive cross section



The contribution given by the interference term and MEC currents turns out to be sizable in the *dip* region.

$e^- - {}^{12}\text{C}$ inclusive cross section



The contribution given by the interference term and MEC currents turns out to be sizable in the *dip* region.

The GFMC approach

Accurate calculations of the electromagnetic responses of ^4He and ^{12}C has been recently performed within GFMC. Nuclear correlations are generated by a realistic Hamiltonian and consistent two-body currents are included.

Inversion of the Euclidean response:

$$\tilde{E}_{T,L}(\mathbf{q}, \tau) = \int_{\omega_{e1}}^{\infty} d\omega e^{-\omega\tau} R_{T,L}(\mathbf{q}, \omega) .$$

$$\tilde{E}_L(\mathbf{q}, \tau) = \langle 0 | \rho^*(\mathbf{q}) e^{-(H-E_0)\tau} \rho(\mathbf{q}) | 0 \rangle - |\langle 0 | \rho(\mathbf{q}) | 0 \rangle|^2 e^{-\omega_{e1}\tau} ,$$

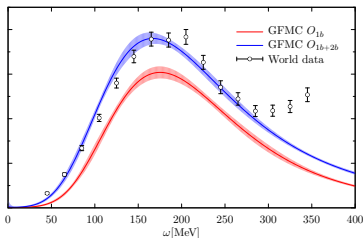
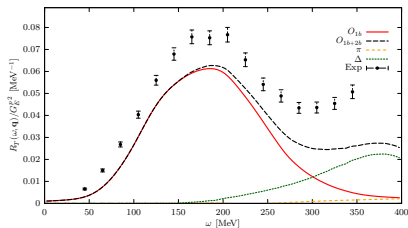
$$\tilde{E}_T(\mathbf{q}, \tau) = \langle 0 | \mathbf{j}_T^\dagger(\mathbf{q}) e^{-(H-E_0)\tau} \mathbf{j}_T(\mathbf{q}) | 0 \rangle - |\langle 0 | \mathbf{j}_T(\mathbf{q}) | 0 \rangle|^2 e^{-\omega_{e1}\tau} ,$$

$$\rho_i(\mathbf{q}) = \left[\frac{G_{E,i}(Q^2)}{\sqrt{1 + Q^2/(4m^2)}} - i \frac{(2G_{M,i}(Q^2) - G_{E,i}(Q^2))}{4m^2} \mathbf{q} \cdot (\boldsymbol{\sigma}_i \times \mathbf{p}_i) \right] .$$

$$\mathbf{j}_i^T(\mathbf{q}) = \left[\frac{G_{E,i}(Q^2)}{m} \mathbf{p}_i^T - i \frac{G_{M,i}(Q^2)}{2m} \mathbf{q} \times \boldsymbol{\sigma} \right] ,$$

Different results obtained within GFMC and SF approach

^{12}C $q=570$ MeV

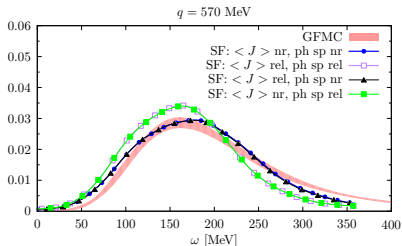
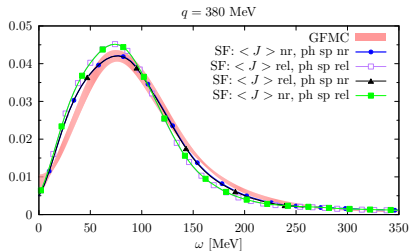
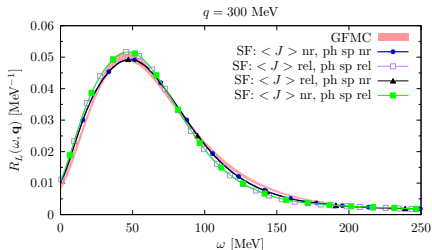


A. Lovato et al, Phys. Rev. Lett.117, 082501

These differences should be ascribed to...

- The non relativistic nature of the GFMC calculations
- Interference between amplitudes involving the one- and two-body currents and $1p1h$ final states
- Differences in the two-nucleon currents employed in the two cases

$R_L(\omega, q)$ of ^{12}C within GFMC and SF approaches



Nice agreement between the SF and GFMC calculation in the longitudinal channel.

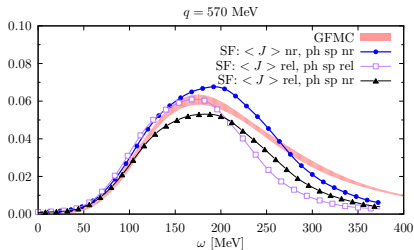
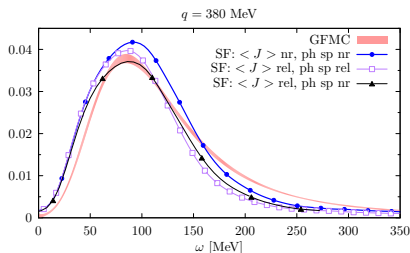
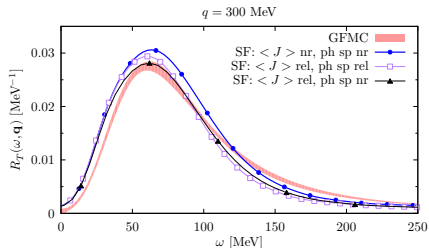
Four different curves labelled SF different

combinations: \star relativistic - non relativistic currents

\star relativistic - non relativistic δ -function

arXiv:1610.06081

$R_T(\omega, q)$ of ^{12}C within GFMC and SF approaches

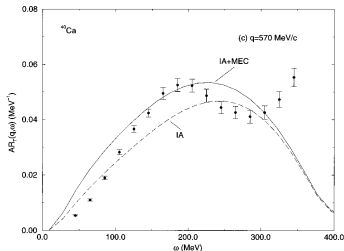


SF: we are neglecting the matrix element of the current containing terms linear in the momentum of the struck particle.

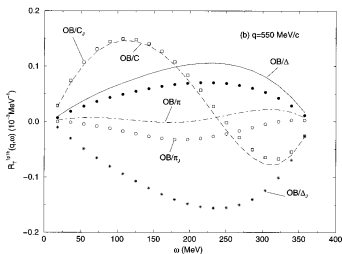
GFMC: the non relativistic expansion should be improved with the inclusion of terms $O[(|q|/m)^2]$

arXiv:1610.06081

Analysis of the MEC contributions in the QE peak



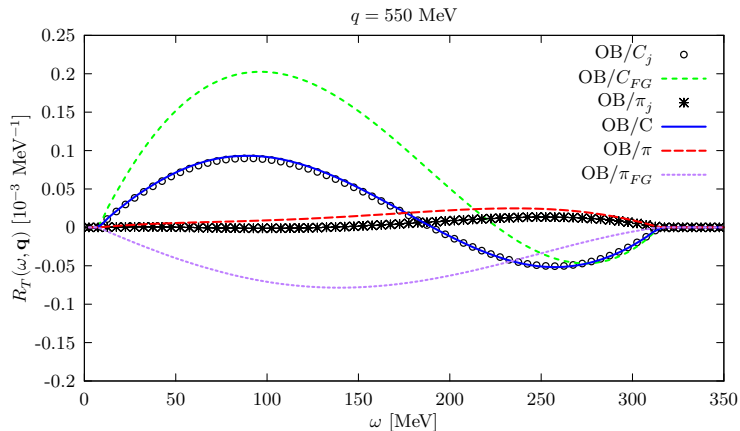
Significant enhancement from two-body current contributions in the region of the quasi-elastic peak this is due to correlated 1p1h final states



The tensor-isospin-dependent correlations drastically modify the behavior of the two-body contribution, which becomes positive and increases with the momentum transfer

A. Fabrocini, Phys. Rev. C 35, 338 (1996)

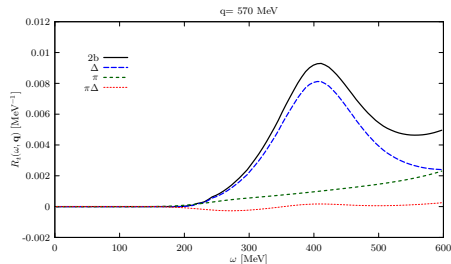
Analysis of the MEC contributions in the QE peak



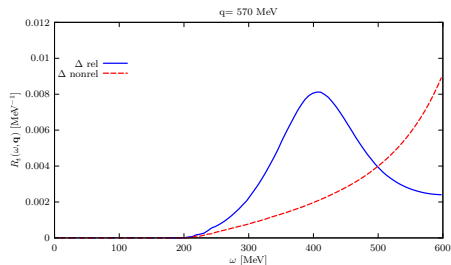
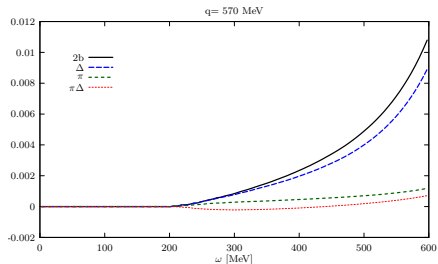
We computed the interference between the **one-body** and the **seagull-** and **pion-in-flight** currents leading to the production of **1p1h final states**. The results we found for the nuclear matter transverse response are in good agreement with the results found by A. Fabrocini.

The impact of relativistic effects in the two-body response

Relativistic



Non relativistic



The most important effect introduced by relativity is the peak produced by the dynamic Δ -propagation

Scaling features of the GFMC results

Scaling of the first kind: the nuclear responses divided by an appropriate function describing the single-nucleon physics no longer depend on the two variables \mathbf{q} and ω , but only upon $\psi(\mathbf{q}, \omega)$.

Relativistic case

$$f_{L,T}(\psi) = p_F \times \frac{R_{L,T}}{G_{L,T}},$$

where

$$\psi = \frac{1}{\sqrt{\xi_F}} \frac{\lambda - \tau}{\sqrt{(1 + \lambda)\tau + \kappa\sqrt{\tau(1 + \tau)}}}$$

Non relativistic case

$$f_{L,T}^{nr}(\psi^{nr}) = p_F \times \frac{R_{L,T}^{nr}}{G_{L,T}^{nr}},$$

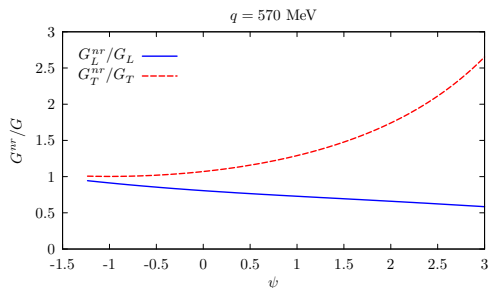
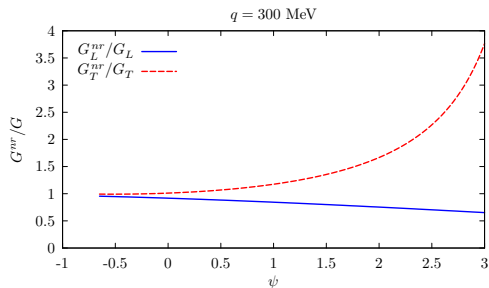
where

$$\psi^{nr} = \frac{1}{\sqrt{2\xi_F^{nr}}} \left(\frac{\lambda}{\kappa} - \kappa \right).$$

Within the GRFG model we obtain ...

$$f(\psi) = f_L(\psi) = f_T(\psi) = \frac{3\xi_F}{2\eta_F^2} (1 - \psi^2)\theta(1 - \psi^2).$$

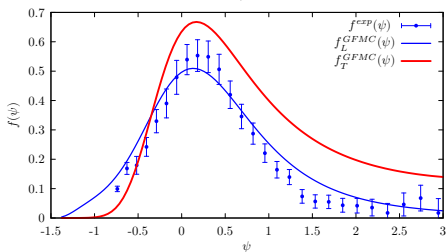
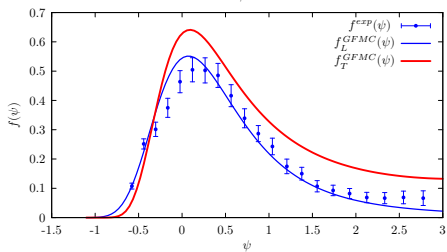
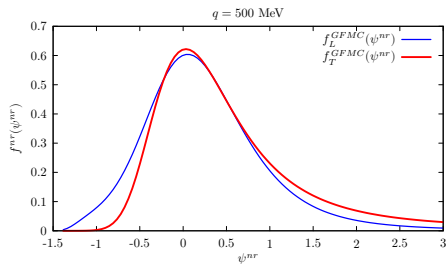
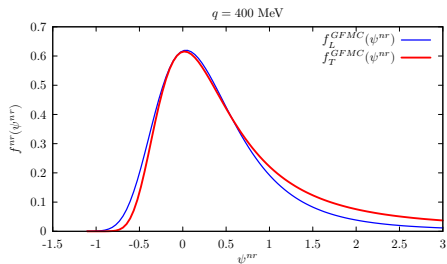
Different behaviour of the prefactors



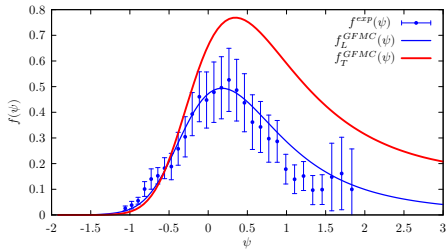
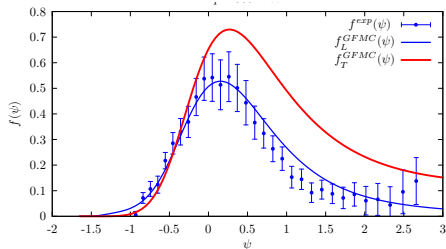
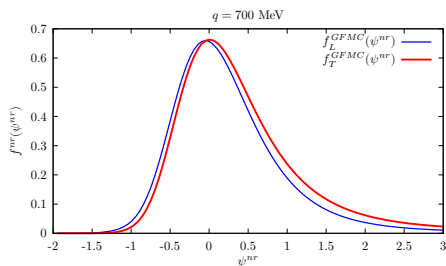
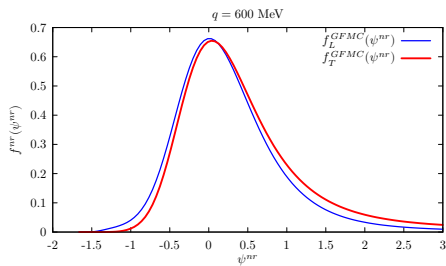
Relativistic effects are particularly relevant in the transverse case; the ratio G_T^{nr}/G_T significantly differs from 1 for $\psi \geq -0.5$.

To highlight the nuclear dynamics we first divide the GFMC results by $G_{L,T}^{nr}$.

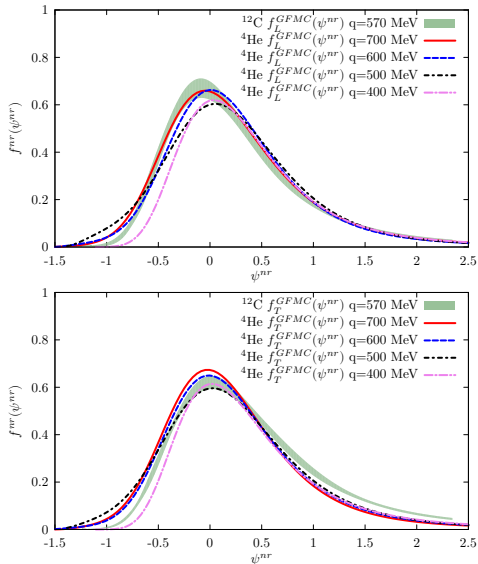
Longitudinal and transverse scaling functions of ^4He within GFMC approach



Longitudinal and transverse scaling functions of ^4He within GFMC approach



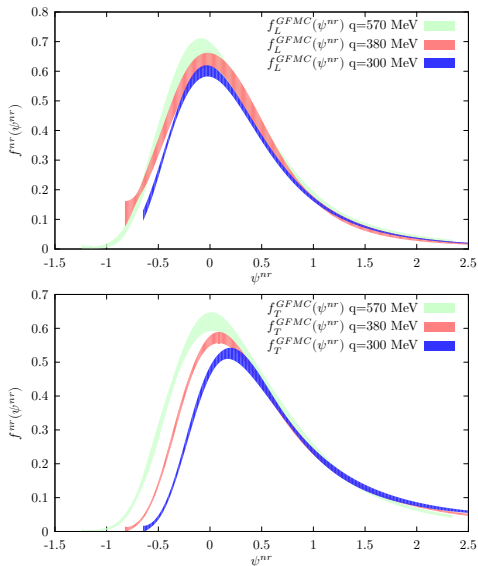
Longitudinal and transverse scaling functions of ^4He within GFMC approach



Note that...

- Scaling of the first-kind is clearly visible when the effects of nuclear dynamics are singled out
- Asymmetric shape of the scaling functions, for all the values of the momentum transfer

Longitudinal and transverse scaling functions of ^{12}C within GFMC approach



First-kind scaling occurs. However, the interpretation of the differences between the three curves is made difficult by the residual effect of the low-lying transition which affect the ^{12}C longitudinal responses. A more meaningful comparison is provided by the results in the transverse channel.

Novel interpretation of the scaling function

The longitudinal scaling function corresponds to the nucleon-density response:

$$f_L = \frac{2\kappa R_\rho}{\mathcal{N}}$$

where R_ρ is the nucleon-density response function defined as

$$R_\rho \equiv \sum_f \langle 0 | \rho^\dagger(\mathbf{q}) | f \rangle \langle f | \rho(\mathbf{q}) | 0 \rangle \delta(E_0 + \omega - E_f),$$

In the transverse channel, for $|\mathbf{q}| \gg 1$ the term $\propto |\mathbf{p}_T|$ can be safely neglected and the scaling function is proportional to the spin-response. In the IA the spin-response reduces to the nucleon-density response.

The two-body current contribution leads to an enhancement of R_T . The inclusion of this contribution in the scaling analysis is likely to explain the scaling violations in the transverse channel.

Novel interpretation of the scaling function

The longitudinal scaling function corresponds to the nucleon-density response:

$$f_L = \frac{2\kappa R_\rho}{\mathcal{N}}$$

where R_ρ is the nucleon-density response function defined as

$$R_\rho \equiv \sum_f \langle 0 | \rho^\dagger(\mathbf{q}) | f \rangle \langle f | \rho(\mathbf{q}) | 0 \rangle \delta(E_0 + \omega - E_f),$$

In the transverse channel, for $|\mathbf{q}| \gg 1$ the term $\propto |\mathbf{p}_T|$ can be safely neglected and the scaling function is proportional to the spin-response. In the IA the spin-response reduces to the nucleon-density response.

The two-body current contribution leads to an enhancement of R_T . The inclusion of this contribution in the scaling analysis is likely to explain the scaling violations in the transverse channel.

Novel interpretation of the scaling function

The longitudinal scaling function corresponds to the nucleon-density response:

$$f_L = \frac{2\kappa R_\rho}{\mathcal{N}}$$

where R_ρ is the nucleon-density response function defined as

$$R_\rho \equiv \sum_f \langle 0 | \rho^\dagger(\mathbf{q}) | f \rangle \langle f | \rho(\mathbf{q}) | 0 \rangle \delta(E_0 + \omega - E_f),$$

In the transverse channel, for $|\mathbf{q}| \gg 1$ the term $\propto |\mathbf{p}_T|$ can be safely neglected and the scaling function is proportional to the spin-response. In the IA the spin-response reduces to the nucleon-density response.

The two-body current contribution leads to an enhancement of R_T . The inclusion of this contribution in the scaling analysis is likely to explain the scaling violations in the transverse channel.

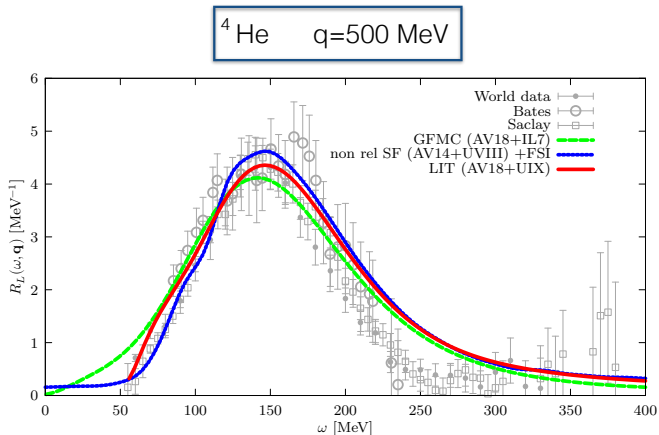
- ▶ An accurate analysis of the role played by the interference between amplitudes involving the one- and two-body currents and 1p1h final states is currently being carried out.
- ▶ The implementation of our results in the determination of the nuclear response to electroweak probes will require the introduction of the one- and two-nucleon axial currents. This is crucial for a correct data analysis of neutrino oscillation experiments (T2K, MiniBooNE, MINERvA ...)
- ▶ The technology based on Liquid Argon Time Projection Chambers (LAr-TPC), will be largely exploited by future experiments, such as DUNE, designed to carry out high-precision measurements of ν oscillations. This will require an extension of the spectral function formalism



Thank you!

backup slides

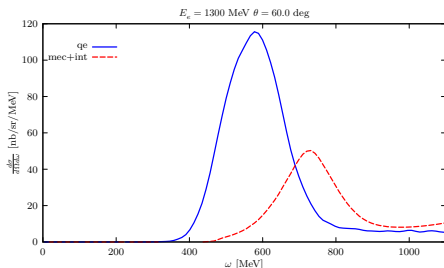
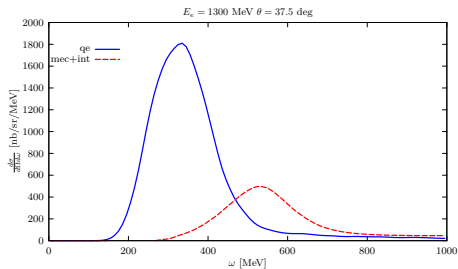
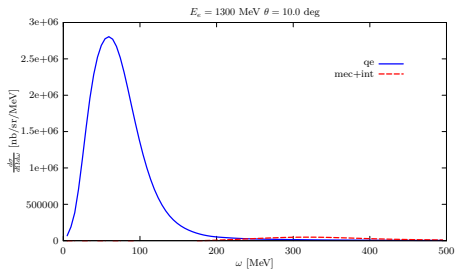
Comparison of the results for the R_L of ${}^4\text{He}$



Good agreement. . .

The spread of the three curves is significantly smaller than
the experimental errorbars

Angular dependence of the two-body contribution



The relative strength due to two-body processes increases for larger values of the scattering angle where the transverse response becomes dominant .

Exact ^4He spectral function in a semirealistic NN potential model

Victor D. Efros,¹ Winfried Leidemann,^{2,3} and Giuseppina Orlandini^{2,3}

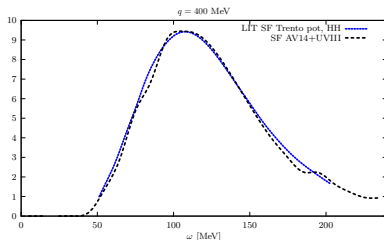
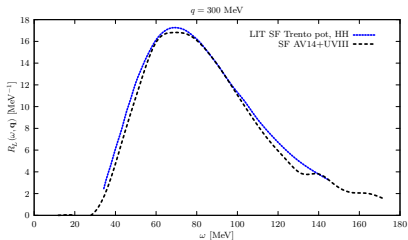
¹Russian Research Centre "Kurchatov Institute," Kurchatov Square 1, 123182 Moscow, Russia

²Dipartimento di Fisica, Università di Trento, I-38050 Povo (Trento), Italy

³Istituto Nazionale di Fisica Nucleare, Gruppo collegato di Trento, Italy

(Received 18 November 1997)

These results refer to a PWIA calculation \rightarrow FSI neglected



Convolution approach

$$S(\mathbf{q}, \omega) = \int d\omega' S_0(\mathbf{q}, \omega) f_{\mathbf{q}}(\omega - \omega')$$

This expression can be obtained in a consistent fashion with a more fundamental approach

The Response of a system can be written in terms of the p-h propagator

$$S(\mathbf{q}, \omega) = \frac{1}{\pi} \text{Im} \Pi(\mathbf{q}, \omega) = \frac{1}{\pi} \text{Im} \left[\langle 0 | \rho_{\mathbf{q}}^{\dagger} \frac{1}{H - E_0 - \omega - i\epsilon} \rho_{\mathbf{q}} | 0 \rangle \right]$$

In the limit of large momentum transfer, where the effect of long range correlations can be neglected,

$\Pi(\mathbf{q}, \omega)$ can be written in terms of the p-h Green's functions.

Final State Interaction in the SF formalism

$$S(\mathbf{q}, \omega) = \int d^3k dE P_h(\mathbf{k}, E) P_p(\mathbf{k} + \mathbf{q}, \omega - E)$$

Within the IA, where FSI are neglected

$$S_0(\mathbf{q}, \omega) = \int d^3k dE P_h(\mathbf{k}, E) \theta(|\mathbf{k} + \mathbf{q}| - k_F) \delta(\omega - E - E_{\mathbf{k}+\mathbf{q}})$$

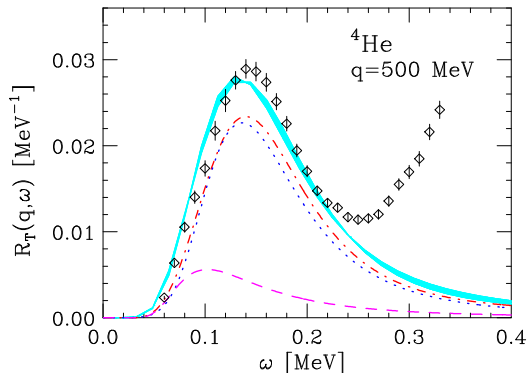
Collecting together the above results, the p-SF can be written as

$$P_p(\mathbf{k} + \mathbf{q}, \omega - E) = \theta(|\mathbf{k} + \mathbf{q}| - k_F) \int d\omega' f_{\mathbf{q}}(\omega - \omega') \delta(\omega' - E - E_{\mathbf{k}+\mathbf{q}})$$

and if we assume: $k + q \sim q$, $E_{\mathbf{k}+\mathbf{q}} \sim E_{\mathbf{q}}$

$$f_{\mathbf{q}}(\omega) = P_p(\mathbf{q}, \omega + E_{\mathbf{q}})$$

The relevance of the interference term. . . $R_T(q, \omega)$



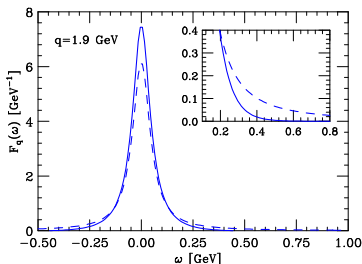
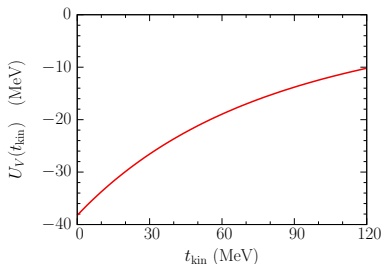
- ▶ Green's Function Monte Carlo calculation of the transverse electromagnetic response function of ${}^4\text{He}$.
- ▶ MEC significantly enhance the transverse response function, not only in the dip region, but also in the quasielastic peak and threshold regions.

Inclusion of Final State Interaction contribution

- ▶ $f_{\mathbf{q}}(\omega - \omega' - U_V)$
- ▶ We consider $T_A = T_A(t_{kin})$ and $U_V = U_V(t_{kin})$ where

$$t_{kin} = \frac{E_k^2(1 - \cos\theta)}{M + E_K(1 - \cos\theta)}$$

- ▶ $F_{\mathbf{q}}(\omega)$ at $|\mathbf{q}| \sim 2$ GeV, including NN correlations



- A. Ankowski *et al.*, Phys. Rev. D 91, 033005 (2015)
- O. Benhar, Phys. Rev. C 87, 024606 (2013).

Extraction of the argon spectral function from $(e, e'p)$ data

- ▶ The spectral function will be obtained combining electron scattering data and the results of theoretical calculations, within the framework of the Local Density Approximation (LDA) \Rightarrow **dedicated electron scattering experiment at JLab**
- ▶ Achieving this goal will require a careful analysis of the measured $(e, e'p)$ cross section as well as the extension of the existing studies of the nuclear matter spectral function to the case of a two-component system, needed to describe non isospin-symmetric matter.

The relevance of the interference term... Sum Rule

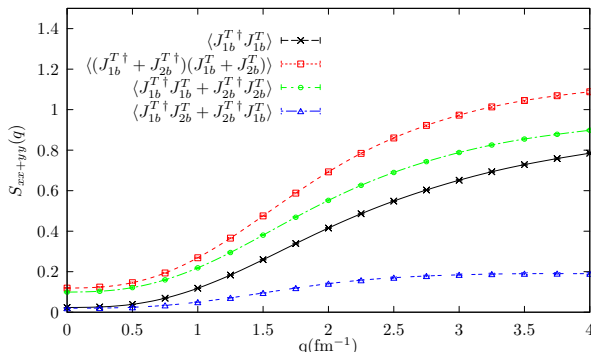
- Sum rule of the electromagnetic response in the T channel

$$S_T(\mathbf{q}) = \int d\omega S_T(\mathbf{q}, \omega), \quad S_T(\mathbf{q}, \omega) = S^{xx}(\mathbf{q}, \omega) + S^{yy}(\mathbf{q}, \omega),$$

where

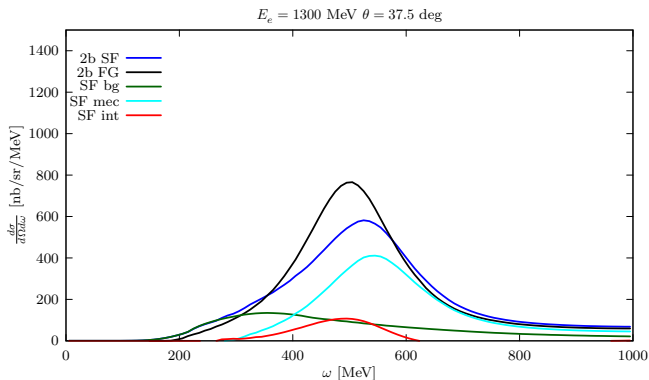
$$\blacktriangleright S^{\alpha\beta} = \sum_N \langle 0 | J_A^\alpha | N \rangle \langle N | J_A^\beta | 0 \rangle \delta(E_0 + \omega - E_N)$$

- Need for a consistent treatment of *both* correlations and MEC currents.



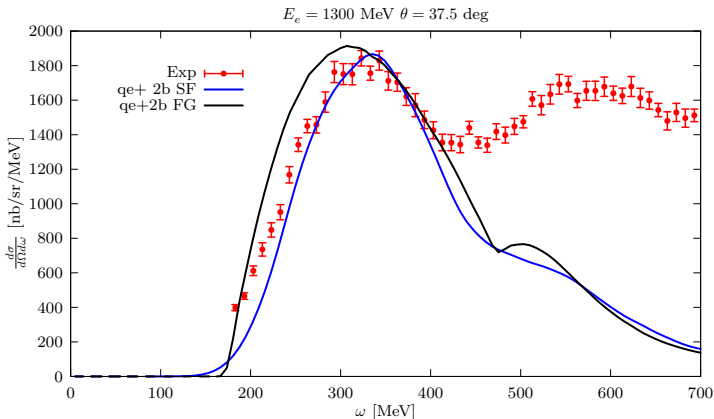
Two-body contribution within the SF and FG formalism

The introduction of the two-nucleon current contributions in theoretical approaches based on the independent particle model (IPM) of nuclear structure, provides a quantitative wealth of the experimental data.



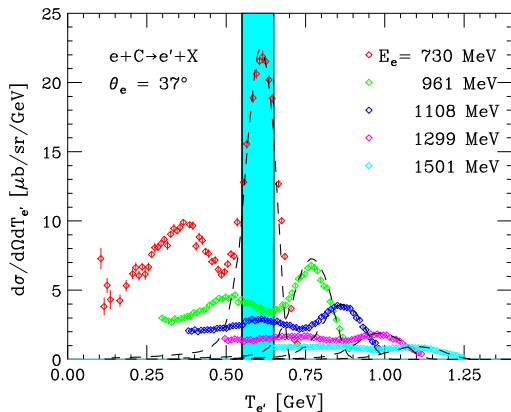
- The total two-body contribution obtained within the SF formalism do not differs too much from the FG result.

e^- - ^{12}C cross section within the SF and FG formalism



- While there are sizable differences both in the position and width of the QE peak, in the “dip” region the results obtained for the e^- - ^{12}C cross section within the SF and FG approaches do not differ significantly.

"Flux averaged" QE electron-Carbon cross section



- Electron-Carbon scattering cross sections at $\theta_e = 37^\circ$ plotted as a function of $T_{e'}$.
- Reaction mechanisms other than single-nucleon knockout contribute to the "flux-averaged" cross section.

- ▶ development of models based on a **new paradigm**, in which all relevant reaction mechanisms are *consistently* taken into account within a unified description of nuclear dynamics.

- The hadronic tensor can be written in the simple form

$$W_A^{\mu\nu} = \int d^3p dE P(\mathbf{p}, E) \frac{M}{E_p} [Z W_p^{\mu\nu} + (A - Z) W_n^{\mu\nu}] ,$$

- Elements entering the definition of the IA x-section

- ▶ the tensor describing the interactions of the i -th nucleon in free space

$$W_\alpha^{\mu\nu} = \sum_X \langle -\mathbf{p}_R, N | j_\alpha^{\mu\dagger} | X, \mathbf{p}_X \rangle \langle X, \mathbf{p}_X | j_\alpha^\nu | -\mathbf{p}_R, N \rangle \delta^{(4)}(\tilde{q} - p_R - p_X) .$$

$$\tilde{\omega} = E_X - \sqrt{\mathbf{p}^2 + M^2} = \omega + M - E - \sqrt{\mathbf{p}^2 + M^2}$$

- ▶ The nucleon energy and momentum distribution, described by the hole spectral functions

Violation of current conservation

The replacement of ω with $\tilde{\omega}$ leads to a violation of the current conservation:

$$q_\mu w_N^{\mu\nu} = 0$$

Prescription proposed by *de Forest*:

$$\tilde{w}_N^{\mu\nu} = w_N^{\mu\nu}(\tilde{q})$$

$$\tilde{w}_N^{3\nu} = \frac{\omega}{|\mathbf{q}|} w_N^{0\nu}(\tilde{q})$$

The violation of gauge invariance only affects the longitudinal response. As a consequence, it is expected to become less and less important as the momentum transfer increases, electron scattering at large $|\mathbf{q}|$ being largely dominated by transverse contributions.

Local Density Approximation (LDA) $P(\mathbf{k}, E)$ for oxygen

$$P_{LDA}(\mathbf{p}, E) = P_{MF}(\mathbf{p}, E) + P_{\text{corr}}(\mathbf{p}, E)$$

- $P_{MF}(\mathbf{p}, E) \rightarrow$ from $(e, e'p)$ data
- $P_{\text{corr}}(\mathbf{p}, E) \rightarrow$ from uniform nuclear matter calculations at different densities:

$$P_{MF}(\mathbf{p}, E) = \sum_{n \in \{F\}} Z_n |\phi_n(\mathbf{p})|^2 F_n(E - E_n)$$

$$P_{\text{corr}}(\mathbf{p}, E) = \int d^3r \varrho_A(\mathbf{r}) P_{\text{corr}}^{NM}(\mathbf{p}, E; \varrho = \varrho_A(\mathbf{r}))$$

Hadronic monopole form factors

$$\begin{aligned} F_{\pi NN}(k^2) &= \frac{\Lambda_\pi^2 - m_\pi^2}{\Lambda_\pi^2 - k^2} \\ F_{\pi N\Delta}(k^2) &= \frac{\Lambda_{\pi N\Delta}^2}{\Lambda_{\pi N\Delta}^2 - k^2} \end{aligned} \quad (1)$$

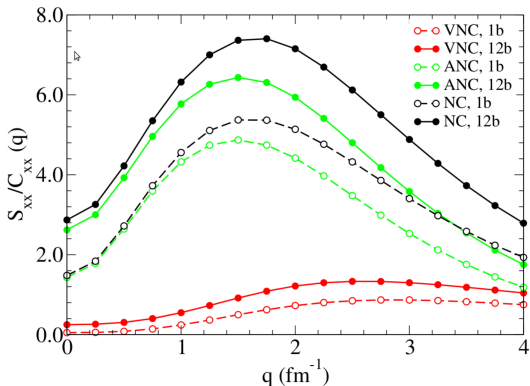
and the EM ones

$$\begin{aligned} F_{\gamma NN}(q^2) &= \frac{1}{(1 - q^2/\Lambda_D^2)^2} , \\ F_{\gamma N\Delta}(q^2) &= F_{\gamma NN}(q^2) \left(1 - \frac{q^2}{\Lambda_2^2}\right)^{-1/2} \left(1 - \frac{q^2}{\Lambda_3^2}\right)^{-1/2} \end{aligned} \quad (2)$$

where $\Lambda_\pi = 1300$ MeV, $\Lambda_{\pi N\Delta} = 1150$ MeV, $\Lambda_D^2 = 0.71 \text{GeV}^2$,
 $\Lambda_2 = M + M_\Delta$ and $\Lambda_3^2 = 3.5 \text{GeV}^2$.

Neutral weak current two-body contributions

The enhancement due to two-nucleon currents, at $q \simeq 1 \text{ fm}^{-1}$, is about 50% relative to the one-body values.

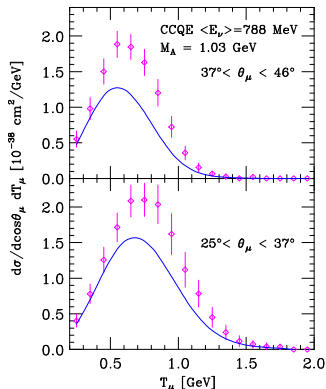
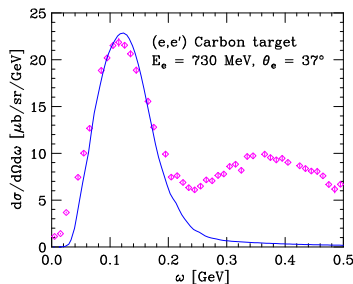


- ▶ Low momentum transfer the dominant contribution is given by: $\langle ij_{2b}^\dagger j_{2b} | i \rangle$
- ▶ At higher momentum transfer: $\langle ij_{2b}^\dagger j_{1b} | i \rangle + \langle ij_{1b}^\dagger j_{2b} | i \rangle$ plays a more important role.

- ▶ A.Lovato *et al.*, Phys. Rev. Lett. 112, 182502 (2014)

- Data: MiniBooNE Collaboration

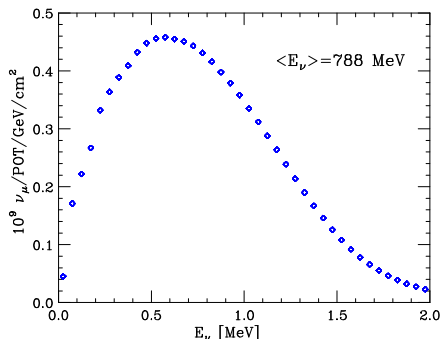
- Data: J.S. O'Connell *et al*



- The calculations performed using the spectral function and the measured nuclear vector form factors accurately reproduce the QE peak measured in electron scattering
- The same scheme largely fails to explain the MiniBooNE data.

QE neutrino-nucleus scattering

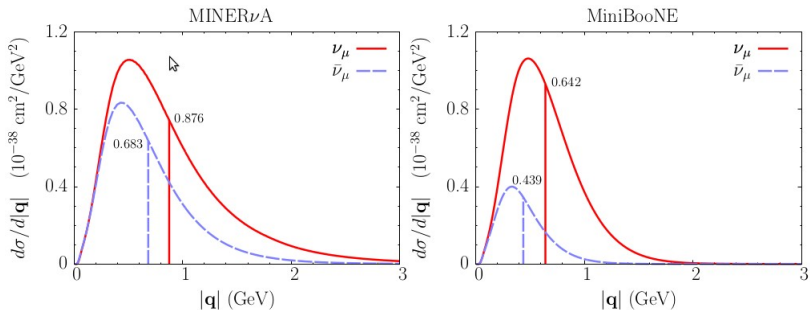
- ▶ The measured double differential CCQE cross section is averaged over the neutrino flux



- ▶ Energy distribution of MiniBooNE neutrino flux
- ▶ Different reaction mechanisms contribute to the cross section at fixed θ_μ and T_μ .

A description of neutrino-nucleus interactions, has to be validated through extensive comparison to the large body of electron-nucleus scattering data.

Kinematical range of accelerator-based neutrino experiments



- $|q|$ -dependence of CCQE cross section averaged with the MinervA and MiniBooNE fluxes

WARNING!

unlike the ground state, **the nuclear current operator and the nuclear final state depend on momentum transfer**. At large q non relativistic approximations become inadequate.

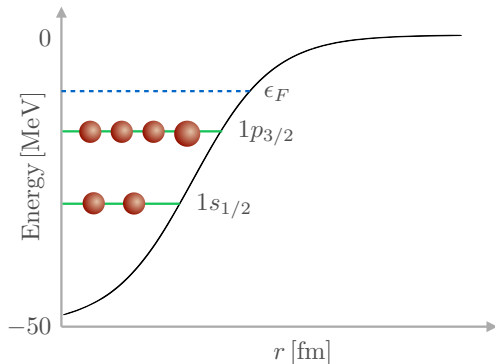
2p-2h Transverse Response of ^{12}C

Set of Harmonic Oscillator wave functions

$$\Psi_{0,0,0}(r) \Leftrightarrow \alpha = 1$$

$$\Psi_{0,1,1}(r) \Leftrightarrow \alpha = 2$$

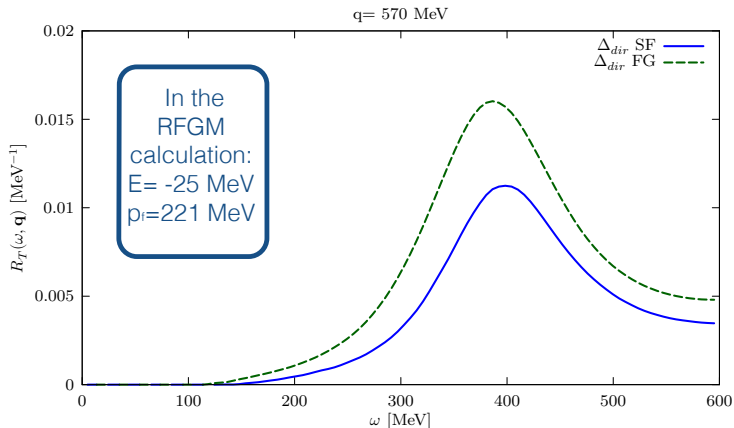
$$\Psi_{0,1,-1}(r) \Leftrightarrow \alpha = 3$$



$$P_{2h}(\mathbf{k}, \mathbf{k}', E) = \sum_{\alpha_1, \alpha_2=1}^3 Z_{\alpha_1} Z_{\alpha_2} |\Psi_{\alpha_1}(k)|^2 |\Psi_{\alpha_2}(k')|^2 F(E + e_{\alpha_1}(k) + e_{\alpha_2}(k'))$$

$$e_1 = -38 \text{ MeV}, \quad e_{2,3} = -17.0 \text{ MeV} \quad Z_1 = 0.5, \quad Z_{2,3} = 0.625$$

Beyond the RFGM ...



Sizable differences

Different threshold \Rightarrow different treatment of the initial state energies of the knocked-out nucleons.

Significant quenching of the response \Rightarrow short range correlations.